DOI: 10.1002/ejic.200900674

Dimeric Nickel(II) Containing Tungstogermanate $[\{\beta\text{-}GeNi_2W_{10}O_{36}(OH)_2(H_2O)\}_2]^{12-}$

Nadeen H. Nsouli,[a] Manuel Prinz,[b] Niklas Damnik,[b] Manfred Neumann,*[b] Ewa Talik,[c] and Ulrich Kortz*[a]

Keywords: Polyoxometalates / Tungsten / Nickel / Magnetic properties

Interaction of the dilacunary polyanion precursor $[\gamma\text{-}GeW_{10}O_{36}]^{8-}$ with Ni^{2+} ions in aqueous medium (pH 5.5) resulted in the formation of the dimeric, tetranickel(II)-containing 20-tungsto-2-germanate $[\{\beta\text{-}GeNi_2W_{10}O_{36}(OH)_2(H_2O)\}_2]^{12-}$ (**1**). Polyanion **1** is composed of two lacunary (β-$GeW_{10}O_{37}$) units accommodating two Ni^{2+} ions each and linked through two triply bridging OH groups. Single-crystal X-ray analysis was carried out on $K_{10}Ni[\{\beta\text{-}GeNi_2W_{10}O_{36}(OH)_2(H_2O)\}_2]\cdot 28H_2O$ (KNi-**1**), which crystallizes in the triclinic system. The title compound KNi-**1** was characterized by IR spectroscopy, elemental analysis, single-crystal XRD, thermogravimetric analysis, and X-ray photoelectron spectroscopy. Magnetization measurements on KNi-**1** revealed that the title polyanion **1** exhibits an antiferromagnetically coupled Ni_4 core.

Introduction

In recent years, polyoxometalates (POMs) have attracted much attention in different areas of science due to their unique tuneable properties, including composition, size, shape, charge density, redox potentials, and solubility.[1] POMs are usually composed of edge- and corner-shared MO_6 octahedra with M being an early d-block metal in a high oxidation state (e.g., W^{VI}, V^{V}). Controlled base hydrolysis can lead to the removal of one or more MO_6 octahedra, resulting in the formation of "lacunary" or "defect" species. For instance, the Keggin polyanion of the general formula $[XM_{12}O_{40}]^{n-}$ (X being the central heteroatom)[2] can lose one, two, or three MO_6 octahedra to form mono-, di-, or trilacunary derivatives, respectively. Such lacunary POM precursors can be considered as inorganic polydentate ligands, which can be reacted with a large variety of electrophiles. POM synthesis is in general not trivial, as a detailed mechanistic understanding is still lacking. Nevertheless, the global interest in POMs is now larger than ever, which is mostly due to a unique combination of attractive properties resulting in potential applications in many different areas including industrial catalysis, magnetic devices, renewable energy science, and medicine.[3]

POMs can be functionalized by incorporation of transition metals, lanthanides, organometallic entities, and so on. One of the major subclasses in POM chemistry is represented by transition-metal-substituted polyoxometalates (TMSPs). The quest to discover novel TMSPs by the reaction of stable lacunary polytungstate precursors with a variety of transition-metal ions under different conditions is an attractive goal, as such derivatives are of particular importance in oxidation catalysis and molecular magnetism. The large number of known TMSPs originates from the diverse structural and compositional types of lacunary POM precursors, such as monovacant α-/β-$[XW_{11}O_{39}]^{8-}$ (X = Si, Ge),[4a,4c] divacant γ-$[XW_{10}O_{36}]^{8-}$ (X = Si, Ge),[4d] trivacant α-/β-$[XW_9O_{34}]^{n-}$ (n = 10, X = Si^{IV}, Ge^{IV}; n = 9, X = P^{V}, As^{V}),[4c,4g] α-$[XW_9O_{33}]^{9-}$ (X = As^{III}, Sb^{III}, Bi^{III}),[4h,4j] α-$[P_2W_{17}O_{61}]^{10-}$,[4k,4l] and hexavacant α-$[H_2P_2W_{12}O_{48}]^{12-}$.[4m,4n] Sandwich-type polyanions constitute a large subclass of TMSPs, and they include species based on two B-α-(XW_9O_{34}) or B-α-$(X_2W_{15}O_{56})$ fragments (Weakley-type),[5] two α-/β-(XW_9O_{34}) fragments (Knoth-type),[6] two B-α-(XW_9O_{33}) fragments (Hervé-type),[7] and two B-β-(XW_9O_{33}) fragments (Krebs-type).[8]

POMs with several exchange-coupled paramagnetic metal ions (e.g., Mn^{2+}, Fe^{3+}, Co^{2+}, Ni^{2+}) are particularly important from a magnetic point of view. To date, several nickel(II)-containing tungstogermanates and -silicates have been reported, such as $[Ni_4(H_2O)_2(GeW_9O_{34})_2]^{12-}$,[9] $[Ni_4(H_2O)_2(SiW_9O_{34})_2]^{10-}$,[10] $[Ni_6(\mu_3\text{-}OH)_3(H_2O)_6(enMe)_3(B\text{-}\alpha\text{-}SiW_9O_{34})]^{-}$,[11] $[\{Ni_6(\mu_3\text{-}OH)_3(en)_3(H_2O)_6\}(B\text{-}\alpha\text{-}Si-$

[a] School of Engineering and Science, Jacobs University, P.O. Box 750 561, 28725 Bremen, Germany
Fax: +49-421-200-3229
E-mail: u.kortz@jacobs-university.de
[b] University of Osnabrück, Department of Physics, Barbarastr. 7, 49069 Osnabrück, Germany
[c] University of Silesia, Faculty of Mathematics, Physics and Chemistry, 14 Bankowa St., 40-007 Katowice, Poland
Supporting information for this article is available on the WWW under http://dx.doi.org/10.1002/ejic.200900674.

$W_9O_{34})][Ni_{0.5}(en)]$,[12] $[Na\{(A\text{-}\alpha\text{-}SiW_9O_{34})Ni_4(CH_3COO)_3(OH)_3\}_2]^{15-}$, $[Na\{(A\text{-}\alpha\text{-}SiW_9O_{34})Ni_4(CH_3COO)_3(OH)_2(N_3)\}_2]^{15-}$, and $[(A\text{-}\alpha\text{-}SiW_9O_{34})_2Ni_9(OH)_6(H_2O)_6(CO_3)_3]^{14-}$.[13]

Here we report on the synthesis, structural characterization, magnetic studies, and X-ray photoelectron spectroscopy of a dimeric tetranickel(II) containing 20-tungsto-2-germanate.

Results and Discussion

Synthesis and Structure

Reaction of $NiCl_2{\cdot}6H_2O$ with $K_8[\gamma\text{-}GeW_{10}O_{36}]{\cdot}6H_2O$ in a ratio of 6:1 in 1 M KCl solution (pH 5.5) at 50 °C resulted in the dimeric tungstogermanate $[\{\beta\text{-}GeNi_2W_{10}O_{36}(OH)_2(H_2O)\}_2]^{12-}$ (**1**). Polyanion **1** consists of two lacunary ($\beta_{2,3}$-$GeW_{10}O_{37}$) fragments (the subscript "2,3" indicating that one Ni^{2+} ion is located in the rotated triad itself and the other one in the adjacent belt; the precise positions of the two Ni^{2+} ions according to IUPAC are "4,10"),[14] each accommodating two Ni atoms in the defect sites leading to the formation of the complete β-Keggin ion. Both nickel ions are structurally nonequivalent (Ni1 and Ni2), see Figure 1b. The two $[\beta\text{-}GeNi_2W_{10}O_{36}(OH)_2(H_2O)]^{6-}$ Keggin moieties in **1** are linked through the two oxygen atoms O1N2 and O1N2′ (see Figure 1). Each of these oxygen atoms is linked to two nickel centers in the same Keggin unit and to another nickel atom of the second Keggin unit, thus acting as a μ_3-oxido bridge. The two half-units in **1** are related by an inversion center. For O1N2, O1N2′, O10B, and O10B′, the respective summation of bond valences leads to a value of around 1.0, strongly suggesting monoprotonation. The bond valence sum for O1N1 and O1N1′ is equal to 0.37, which indicates that these two oxygen atoms are actually water molecules (see Figure 1). The above is fully consistent with our previously reported $[\{\beta\text{-}SiNi_2W_{10}O_{36}(OH)_2(H_2O)\}]^{12-}$ (**2**), which represents the silicon analogue of **1**.[17] The main differences between **1** and **2** are the respective heteroatom–oxygen bond lengths. The Ge–O bonds in **1** are 1.76(1), 1.74(1), 1.72(1), and 1.76(1) Å [avg. 1.75(1) Å], whereas the Si–O bonds in **2** are 1.60(2), 1.66(2), 1.61(2), and 1.63(2) Å [avg. 1.63(2) Å]. We found 10 K^+ counterions for **1** by XRD, and elemental analysis revealed that the remaining two charges are balanced by a Ni^{2+} countercation. This has, of course, consequences for the magnetic properties of KNi-**1** (vide infra).

Here, it is worth mentioning Enbo Wang's nickel(II)-containing tungstosilicate $[\{Ni_6(H_2O)_4(\mu_2\text{-}H_2O)_4(\mu_3\text{-}OH)_2\}(SiW_9O_{34})_2]^{10-}$, which consists of two ($\beta_{2,2,3}$-$Ni_3SiW_9O_{40}$) Keggin units and hence can be considered as a hexanickel(II) containing analog of **1**.[15] In each of the half-units, one Ni^{2+} ion is situated in the rotated triad and the other two in the belt. The linkage of the two Keggin units is accomplished by edge-sharing of the two nickel ions located in the rotated triads.

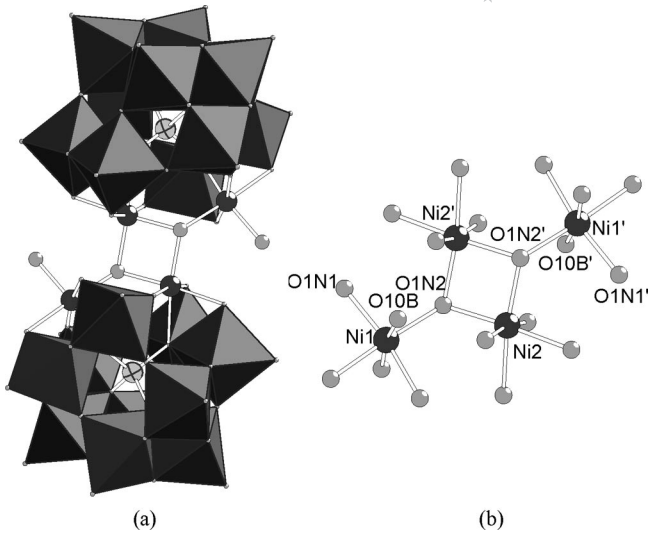

Figure 1. (a) Combined ball-and-stick/polyhedral representation of $[\{\beta\text{-}GeNi_2W_{10}O_{36}(OH)_2(H_2O)\}_2]^{12-}$ (**1**); (b) ball-and-stick representation of the central Ni_4O_{20} unit in **1**. Color code: the balls represent nickel (dark grey), oxygen (light grey), and germanium (light grey, dashed, in the centre of the polyhedra). The polyhedra represent WO_6.

X-ray Photoelectron Spectroscopy

X-ray photoelectron spectroscopy was performed on **1** and its earlier reported Si analogue **2**[17] to clarify the nickel oxidation state and stoichiometry. Figure 2 displays the Ni 2p XP-spectra of KNi-**1** and $K_{12}[\{\beta\text{-}SiNi_2W_{10}O_{36}(OH)_2(H_2O)\}_2]{\cdot}20H_2O$ (K-**2**).

The shapes of the Ni 2p spectra of **1** and **2** exhibit the characteristic features,[17] that is, strong main lines located at 855.7 and 873.5 eV binding energy for the Ni $2p_{3/2}$ and Ni $2p_{1/2}$ peak, respectively, together with a 6.2 eV satellite. The spin–orbit splitting is about 17.5 eV in both spectra, and six regions are observable, labeled A to F. The main Ni $2p_{3/2}$ and Ni $2p_{1/2}$ peaks, labeled A and D, respectively, have a slightly asymmetric shape, whereas the corresponding satellites can each be divided into two regions, labeled B and C for the Ni $2p_{3/2}$ satellite and E and F for the Ni $2p_{1/2}$ satellite.

The shape of the Ni 2p spectrum is due to emission from different configuration states. Thus, the explanations for the peaks (a)–(d) (see Figure 2) are as follows: Peak (a) is due to screening effects, meaning charge transfer effects from oxygen ligands, denoted as electron configuration d^9L^{-1}. Peak (b) is associated with intersite charge transfer effects of neighboring NiO_6 units.[18] Peak (c) corresponds to the unscreened final state. Peak (d) is due to screening effects with two ligand holes.[21]

The absolute binding energy of the Ni $2p_{3/2}$ main line differs (Figure 2b) by about 1.6 eV for the nickel(II)-containing polytungstates and NiO, but due to the fact that the absolute binding energy for the Ni $2p_{3/2}$ peak in NiO varies from 853.6 to 857.2 eV,[19,20] a characteristic shape is observed. The Ni^{2+} ions incorporated in polyanions **1** and **2** exhibit octahedral coordination. The syntheses of **1** and **2**

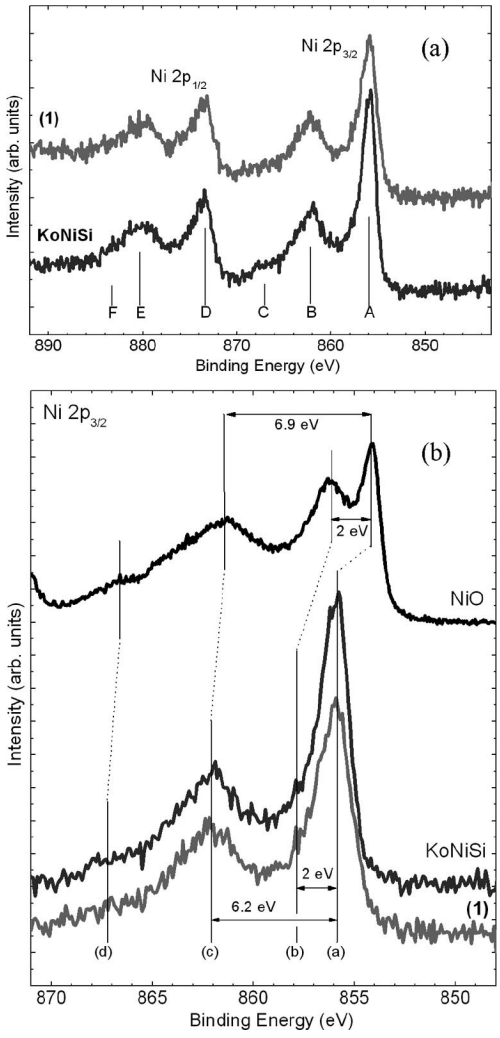

Figure 2. (a) XPS Ni 2p core-level line of KNi-**1** (1) and K-**2** (KoNiSi), for details see text; (b) Ni $2p_{3/2}$ XP-spectra of KNi-**1** (1) and K-**2** (KoNiSi) compared with a Ni $2p_{3/2}$ XP-spectrum of NiO.[16]

were performed by using pure Ni^{2+} salts, and the binding energy difference of Ni metal and Ni^{2+} in **1** and **2** is estimated to be about 2.7 eV.

The stoichiometric analyses (Table 1) were performed by using the MultiPak software and subtracting an Iterated Shirley background from the core-line spectra. The oxygen and carbon concentrations were not considered for the stoichiometry due to adsorbed water and carbon on the sample surface. Only the ratios between tungsten, nickel, and the respective heteroatom (Ge or Si) were determined for polyanions **1** and **2**. Table 1 shows that the Ni/W and Ni/X (X = Ge, Si) ratios are slightly above the expected ones for

Table 1. Atomic concentration ratios (±10%) Ni/W and Ni/X (X = Ge, Si) for KNi-**1** and K-**2**.

	K-**2**[17]		KNi-**1**	
	XPS	expected	XPS	expected
Ni/W	0.22	0.20	0.21	0.20
Ni/X	2.48	2.00	2.25	2.00

both polyanions. The higher Ni contribution (also confirmed by elemental analysis) has an important influence on the magnetic properties, as discussed in the following section.

Magnetic Measurements

Polyanion **1** contains a well-isolated magnetic Ni_4 unit with an interesting geometry. Magnetization measurements allow analyzing the basic magnetic properties of the title compound, that is, the magnetic interactions of the Ni_4 spin cluster. The magnetization measurements for KNi-**1** are displayed in Figure 3. The magnetization at different temperatures between 2 and 100 K were collected in magnetic fields up to 7 T. The magnetization curve of KNi-**1** at 2 K (see Figure 3, top) shows a steep increase up to about 1 T and then starts to curve but without reaching saturation at 7 T, which is similar to the behavior of the compositional analogue K-**2**.[17] Another interesting point is the observation of intersections of the magnetization curves at 2 K with the 4 and 10 K curves at 5.3 and 6.9 T, respectively.

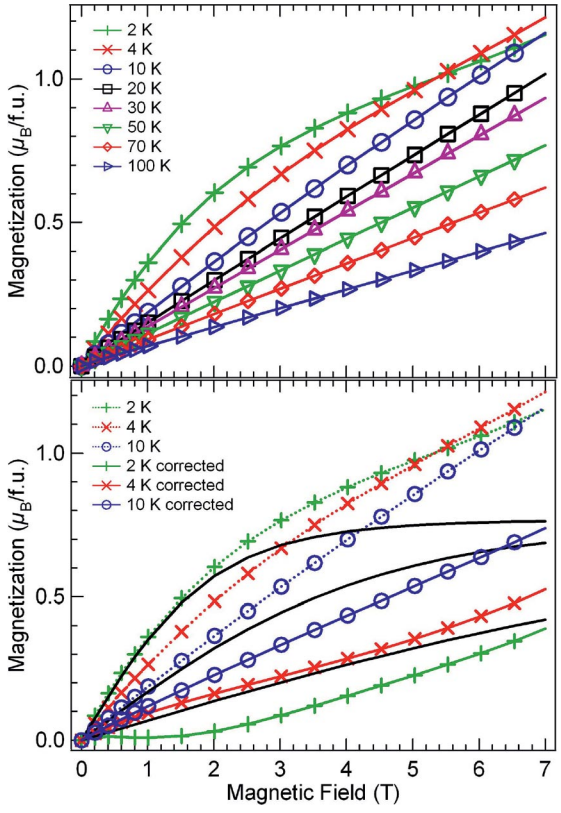

Figure 3. Plot of magnetization of KNi-**1** for different temperatures (top); plot of measured magnetizations at 2, 4, and 10 K (dotted) together with corresponding Brillouin functions (black, solid) and Ni^{2+} countercation impurity corrected magnetization curves (solid; bottom). For details see text.

In order to deal with a possible minor Ni^{2+} countercation impurity for KNi-**1** (vide supra), which would add a paramagnetic contribution to the magnetization, we performed a correction of the magnetization data by subtracting a scaled Brillouin function with $S = 1$ ($Ni^{2+}/3d^8$).

For the sake of completeness, Figure 4 shows a plot of the effective magnetic moment versus temperature for KNi-**1**. Also here strong paramagnetic characteristics, arising from the Ni^{2+} countercation impurity, overlay the weak magnetic interactions of the magnetic core in **1**. This renders understanding of the detailed magnetic interactions in **1** a very difficult task, in particular in the absence of a theoretical model.

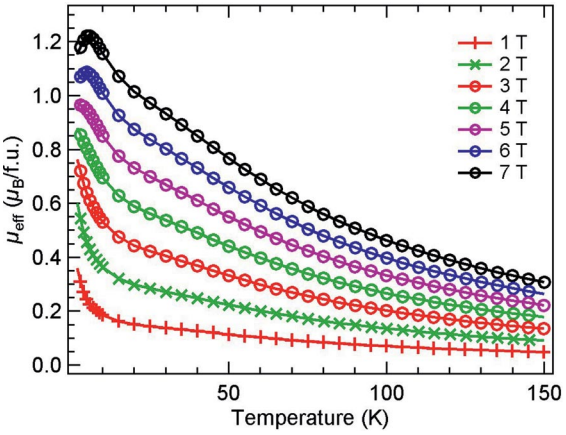

Figure 4. Plot of the effective magnetic moment as a function of temperature for KNi-**1** in various constant magnetic fields.

From stoichiometric analysis of the XPS core-level spectra of KNi-**1** a small deviation of approximately 5% to higher Ni concentrations was found. The subtracted Brillouin function was scaled by a factor of 0.38 to fit under the 2 K magnetization curve (see Figure 3, bottom/2 K curve, dotted, Brillouin function, black), leading to a Ni atomic concentration deviation of approximately 9%. This procedure was also performed for 4 and 10 K, revealing the same factor. The resulting corrected magnetization curves are also shown as colored, solid lines in Figure 3 (bottom).

The observed behavior of the corrected magnetization appears to be antiferromagnetic. Interestingly, at 2 K and a magnetic field below 2 T there is no signal of the antiferromagnetically coupled Ni_4 cluster. Also, the magnetic field of the 2 and 4 K curve intersection has shifted to higher magnetic field, but could still be observed.

Conclusions

We have prepared the dimeric tetranickel(II) containing 20-tungsto-2-germanate $[\{\beta\text{-}GeNi_2W_{10}O_{36}(OH)_2(H_2O)\}_2]^{12-}$ (**1**) by reaction of $NiCl_2{\cdot}6H_2O$ and $K_8[\gamma\text{-}GeW_{10}O_{36}]$ using a simple one-pot reaction in aqueous pH 5.5 medium. Polyanion **1**, which represents the Ge analogue of our $[\{\beta\text{-}SiNi_2W_{10}O_{36}(OH)_2(H_2O)\}_2]^{12-}$ (**2**), was structurally characterized by single-crystal X-ray diffraction, FTIR, and TGA. XPS and magnetic measurements on KNi-**1** are in good agreement and suggest predominantly antiferromagnetic exchange coupling in the Ni_4 spin cluster of **1**.

Experimental Section

Synthesis: All reagents were used as purchased without further purification. The dilacunary precursor $K_8[\gamma\text{-}GeW_{10}O_{36}]$ was synthesized according to the published procedure, and its purity was confirmed by infrared spectroscopy.[19]

$K_{10}Ni[\{\beta\text{-}GeNi_2W_{10}O_{36}(OH)_2(H_2O)\}_2]{\cdot}28H_2O$ (KNi-1): A sample of $K_8[\gamma\text{-}GeW_{10}O_{36}]$ (0.50 g, 0.17 mmol) was added with stirring to a solution of $NiCl_2{\cdot}6H_2O$ (0.27 g, 1.14 mmol) in 1 M KCl (20 mL). The pH was adjusted to 5.5 by using 1 M KOH. The reaction mixture was stirred and heated to 50 °C for 30 min. The solution was allowed to cool to room temperature and then filtered. Slow evaporation of the solvent at room temperature for about one week led to the formation of green crystals suitable for X-ray diffraction. The crystals were isolated and air dried. Yield: 0.08 g, 15%. IR (KBr): $\tilde{\nu}$ = 948 (m), 875 (m), 803 (s), 741 (m), 708 (m), 691 (m), 591 (w), 525 (w), 459 (w), 427 (w) cm^{-1}. $H_{64}Ge_2K_{10}Ni_5O_{106}W_{20}$ (6266.97): calcd. Ge 2.32, H 1.03, K 6.24, Ni 4.68, W 58.7; found Ge 2.46, H 1.12, K 6.23, Ni 4.67, W 57.6.

Instrumentation: Infrared spectra were recorded with a Nicolet Avatar 370 FTIR spectrophotometer using KBr pellets. The following abbreviations were used to assign the peak intensities: w = weak; m = medium; s = strong. Thermogravimetric analyses were carried out on a TA Instruments SDT Q600 thermobalance with a 100 mL min^{-1} flow of nitrogen; the temperature was ramped from room temperature up to 900 °C at a rate of 2 °C min^{-1}. Elemental analyses were performed by Analytische Laboratorien, Lindlar, Germany.

X-ray Crystallography: A single crystal of KNi-**1** was mounted on a Hampton cryoloop in light oil for data collection at –100 °C. Indexing and data collection were performed with a Bruker D8 SMART APEX II CCD diffractometer with kappa geometry and Mo-K_α radiation (graphite monochromator, λ = 0.71073 Å). Data integration was performed using SAINT.[20] Routine Lorentz and polarization corrections were applied. Multiscan absorption correction was performed by using SADABS.[21] Direct methods (SHELXS97) successfully located the tungsten atoms, and successive Fourier syntheses (SHELXL97) revealed the remaining atoms.[16] Refinements were full-matrix least-squares against $|F|^2$ by using all data. In the final refinement, all nondisordered heavy atoms were refined anisotropically; oxygen atoms and disordered cations were refined isotropically. No hydrogen atoms were included in the models. Crystallographic data are summarized in Table 2. Further details of the crystal-structure investigation may

Table 2. Crystal data and structure refinement for KNi-**1**.

Emperical formula	$H_{64}Ge_2K_{10}Ni_5O_{106}W_{20}$
Fw	6267.0
T (K)	173
λ (Å)	0.71073
Space group	$P\bar{1}$
a (Å)	12.4369(6)
b (Å)	12.5548(6)
c (Å)	16.4771(10)
α (°)	99.503(3)
β (°)	97.455(3)
γ (°)	97.316(3)
V (Å^3)	2486.7(2)
Z	1
$d_{calcd.}$ (g cm^{-3})	4.17
Abs. coeff. (mm^{-1})	24.895
R_1 (obsd. data)[a]	0.0472
wR_2 (all data)[b]	0.1355

[a] $R = \Sigma\,||F_o| - |F_c||/\Sigma|F_o|$. [b] $R_w = [\Sigma\, w(F_o^2 - F_c^2)^2/\Sigma w(F_o^2)^2]^{1/2}$.

be obtained from the Fachinformationszentrum Karlsruhe, 76344 Eggenstein-Leopoldshafen, Germany, on quoting the depository number CSD-420850.

X-ray Photoelectron Spectroscopy: The XPS measurements were performed with a PHI 5600ci MultiTechnique XPS System using monochromated Al-K_α radiation ($h\nu$ = 1486.6 eV). The total energy resolution was 0.3–0.4 eV as determined at the Fermi level of a gold foil. As we are studying nonconductive sample charges, neutrality was achieved by supplying low-energy electrons by using a low-energy electron flood gun. The pressure in the UHV main chamber was kept below 5×10^{-9} mbar. The spectra were calibrated after the known position of the C 1s core level line (E_B = 285 eV).

Magnetic Measurements: The SQUID measurements were performed with a Quantum Design MPMS SQUID-Magnetometer. The field dependent magnetization was measured on powder samples of KNi-**1** for the temperatures 1.9, 4.2, 10, 20, and 50 K in magnetic fields up to 7 T. The resulting volume magnetization from the samples had its diamagnetic contribution compensated and was recalculated as volume susceptibility. Diamagnetic contributions were estimated for each compound by using Pascal's constants. Furthermore, the susceptibility measurements were carried out in the temperature range 1.9–300 K in magnetic fields up to 7 T.

Supporting Information (see footnote on the first page of this article): Thermogram of KNi-**1** from room temperature up to 900 °C.

Acknowledgments

U.K. thanks the German Research Council (DFG-KO-2288/4–1), the Fonds der Chemischen Industrie, and Jacobs University for research support. We thank Dr. M. H. Dickman for help with XRD. M.N. acknowledges the PhD program of Lower Saxony for financial support and Prof. J. Schnack (Bielefeld University) for helpful discussions. Figure 1 was generated by Diamond Version 3.2c (copyright Crystal Impact GbR).

[1] a) M. T. Pope in *Heteropoly and Isopoly Oxometalates*, Springer, Berlin, **1983**; b) M. T. Pope, A. Müller, *Angew. Chem. Int. Ed. Engl.* **1991**, *30*, 34–48; c) M. T. Pope in *Comprehensive Coordination Chemistry II* (Eds.: J. A. Meyer, T. J. McCleverty), Elsevier, Oxford, UK, **2004**; d) C. L. Hill in *Comprehensive Coordination Chemistry II* (Eds.: A. G. Wedd), Elsevier, Oxford, UK, **2004**.

[2] J. F. Keggin, *Nature* **1933**, *131*, 908–909.

[3] a) M. T. Pope, A. Müller in *Polyoxometalates: From Platonic Solids to Anti-Retroviral Activity* (Eds.: M. T. Pope, A. Müller), Kluwer, Dordrecht, The Netherlands, **1994**; b) C. L. Hill (Guest Editor), *Chem. Rev.* **1998**, issue 1 (ACS special thematic issue on polyoxometalates); c) M. T. Pope, A. Müller in *Polyoxometalate Chemistry: From Topology via Self-Assembly to Applications* (Eds.: M. T. Pope, A. Müller), Kluwer, Dordrecht, The Netherlands, **2001**; d) T. Yamase, M. T. Pope in *Polyoxometalate Chemistry for Nano-Composite Design* (Eds.: T. Yamase, M. T. Pope), Kluwer, Dordrecht, The Netherlands, **2002**; e) J. J. Borrás-Almenar, E. Coronado, A. Müller, M. T. Pope in *Polyoxometalate Molecular Science* (Eds.: J. J. Borrás-Almenar, E. Coronado, A. Müller, M. T. Pope), Kluwer, Dordrecht, The Netherlands, **2003**; f) M. Vazylyev, D. Sloboda-Rozner, A. Haimov, G. Maayan, R. Neumann, *Top. Catal.* **2005**, *34*, 93–99.

[4] Examples include: a) R. de Paiva Floro Bonfim, L. C. de Moura, H. Pizzala, S. Caldarelli, S. Paul, J. G. Eon, O. Mentre, M. Capron, L. Delevoye, E. Payen, *Inorg. Chem.* **2007**, *46*, 7371–7377; b) M. Sadakane, D. Tsukuma, M. H. Dickman, B. S. Bassil, U. Kortz, M. Higashijima, W. Ueda, *Dalton Trans.* **2006**, 4271–4276; c) Z. Zhang, E. Wang, W. Chen, H. Tan, *Aust. J. Chem.* **2007**, *60*, 284–290; d) U. Kortz, S. Matta, *Inorg. Chem.* **2001**, *40*, 815–817; e) K. Hayashi, M. Takahashi, K. Nomiya, *Dalton Trans.* **2005**, 3751–3756; f) U. Kortz, S. Isber, M. H. Dickman, D. Ravot, *Inorg. Chem.* **2000**, *39*, 2915–2922; g) U. Kortz, S. Nellutla, A. C. Stowe, N. S. Dalal, U. Rauwald, W. Danquah, D. Ravot, *Inorg. Chem.* **2004**, *43*, 2308–2317; h) U. Kortz, N. K. Al-Kassem, M. G. Savelieff, N. A. Al Kadi, M. Sadakane, *Inorg. Chem.* **2001**, *40*, 4742–4749; i) N. Laronze, J. Marrot, G. Hervé, *Inorg. Chem.* **2003**, *42*, 5857–5862; j) U. Kortz, S. Nellutla, A. C. Stowe, N. S. Dalal, J. van Tol, B. S. Bassil, *Inorg. Chem.* **2004**, *43*, 144–154; k) W. J. Randall, T. J. R. Weakley, R. G. Finke, *Inorg. Chem.* **1993**, *32*, 1068–1071; l) U. Kortz, *J. Cluster Sci.* **2003**, *14*, 205–214; m) B. Godin, Y. G. Chen, J. Vaissermann, L. Ruhlmann, M. Verdaguer, P. Gouzerh, *Angew. Chem. Int. Ed.* **2005**, *44*, 3072–3075; n) B. Godin, J. Vaissermann, P. Herson, L. Ruhlmann, M. Verdaguer, P. Gouzerh, *Chem. Commun.* **2005**, 5624–5626.

[5] Examples include: a) T. J. R. Weakley, H. T. Evans Jr., J. S. Showell, G. F. Tourné, C. M. Tourné, *J. Chem. Soc., Chem. Commun.* **1973**, 139–140; b) R. G. Finke, M. W. Droege, *Inorg. Chem.* **1983**, *22*, 1006–1008; c) R. G. Finke, M. W. Droege, P. J. Domaille, *Inorg. Chem.* **1987**, *26*, 3886–3896; d) X.-Y. Zhang, G. B. Jameson, C. J. O'Connor, M. T. Pope, *Polyhedron* **1996**, *15*, 917–922; e) U. Kortz, S. Isber, M. H. Dickman, D. Ravot, *Inorg. Chem.* **2000**, *39*, 2915–2922; f) C. Rosu, D. C. Crans, T. J. R. Weakley, *Polyhedron* **2002**, *21*, 959–962; g) U. Kortz, S. Nellutla, A. C. Stowe, N. S. Dalal, U. Rauwald, W. Danquah, D. Ravot, *Inorg. Chem.* **2004**, *43*, 2308–2317.

[6] Examples include: a) W. H. Knoth, P. J. Domaille, R. D. Farlee, *Organometallics* **1985**, *4*, 62–68; b) W. H. Knoth, P. J. Domaille, R. L. Harlow, *Inorg. Chem.* **1986**, *25*, 1577–1584; c) R. G. Finke, B. Rapko, T. J. R. Weakley, *Inorg. Chem.* **1989**, *28*, 1573–1579; d) F. Xin, M. T. Pope, *J. Am. Chem. Soc.* **1996**, *118*, 7731–7736; e) L.-H. Bi, U. Kortz, B. Keita, L. Nadjo, H. Borrmann, *Inorg. Chem.* **2004**, *43*, 8367–8372.

[7] Examples include: a) F. Robert, M. Leyrie, G. Hervé, *Acta Crystallogr., Sect. B* **1982**, *38*, 358–362; b) U. Kortz, N. K. Al-Kassem, M. G. Savelieff, N. A. Al Kadi, M. Sadakane, *Inorg. Chem.* **2001**, *40*, 4742–4749; c) B. Botar, T. Yamase, E. Ishikawa, *Inorg. Chem. Commun.* **2001**, *4*, 551–554; d) P. Mialane, J. Marrot, E. Rivière, J. Nebout, G. Hervé, *Inorg. Chem.* **2001**, *40*, 44–48; e) U. Kortz, S. Nellutla, A. C. Stowe, N. S. Dalal, J. van Tol, B. S. Bassil, *Inorg. Chem.* **2004**, *43*, 144–154; f) L.-H. Bi, M. Reicke, U. Kortz, B. Keita, L. Nadjo, R. J. Clark, *Inorg. Chem.* **2004**, *43*, 3915–3920.

[8] Examples include: a) M. Bösing, I. Loose, H. Pohlmann, B. Krebs, *Chem. Eur. J.* **1997**, *3*, 1232–1237; b) B. Krebs, E. Droste, M. Piepenbrink, G. Vollmer, *C. R. Acad. Sci. Paris, Ser. IIc* **2000**, *3*, 205–210; c) U. Kortz, M. G. Savelieff, B. S. Bassil, B. Keita, L. Nadjo, *Inorg. Chem.* **2002**, *41*, 783–789; d) E. M. Limanski, D. Drewes, E. Droste, R. Bohner, B. Krebs, *J. Mol. Struct.* **2003**, *656*, 17–25.

[9] Z. Zhang, E. Wang, Y. Li, Y. Qi, H. Tan, *J. Mol. Struct.* **2007**, *843*, 128–131.

[10] X. Zhao, Y.-G. Li, Y.-H. Wang, E. Wang, *Transition Met. Chem.* **2008**, *33*, 323–330.

[11] S.-T. Zheng, D.-Q. Yuan, H.-P. Jia, J. Zhang, G.-Y. Yang, *Chem. Commun.* **2007**, 1858–1860.

[12] J.-W. Zhao, H.-P. Jia, J. Zhang, S.-T. Zheng, G.-Y. Yang, *Chem. Eur. J.* **2007**, *13*, 10030–10045.

[13] C. Pichon, P. Mialane, A. Dolbecq, J. Marrot, E. Rivière, B. S. Bassil, U. Kortz, B. Keita, L. Nadjo, F. Sécheresse, *Inorg. Chem.* **2008**, *47*, 11120–11128.

[14] U. Kortz, Y. P. Jeannin, A. Tézé, G. Hervé, S. Isber, *Inorg. Chem.* **1999**, *38*, 3670–3675.

[15] Z. Zhang, Y. Li, E. Wang, X. Wang, C. Qin, Y. An, *Inorg. Chem.* **2006**, *45*, 4313–4315.

[16] S. Uhlenbrock, *Untersuchungen zur elektronischen Struktur einfacher Übergangsmetalloxide unter besonderer Berücksichtigung*

des Nickeloxides. PhD Thesis, University of Osnabrück, **1994**.
[17] For example: a) H. Kuhlenbeck, G. Odörfer, R. Jaeger, G. Illing, M. Menges, T. Mull, H.-J. Freund, V. Pöhlchen, S. Witzel, C. Scharfschwerdt, K. Wennemann, T. Liedtke, M. Neumann, *Phys. Rev. B* **1991**, *43*, 1969–1986; b) S. Uhlenbrock, C. Scharfschwerdt, M. Neumann, G. Illing, H.-J. Freund, *J. Phys. Cond. Mater.* **1992**, *4*, 7973–7978.
[18] M. A. van Veenendaal, G. A. Sawatzky, *Phys. Rev. Lett.* **1993**, *70*,2459–2462.
[19] N. H. Nsouli, B. S. Bassil, M. H. Dickman, U. Kortz, B. Keita, L. Nadjo, *Inorg. Chem.* **2006**, *45*, 3858–3860.
[20] *SAINT*, Bruker AXS Inc., Madison, Wisconsin, USA, **2007**.
[21] G. M. Sheldrick, *Acta Crystallogr., Sect. A* **2008**, *64*, 112–122.
Received: July 18, 2009
Published Online: October 30, 2009

